HHS Public Access

Author manuscript

Biochem J. Author manuscript; available in PMC 2020 November 15.

Published in final edited form as:

Biochem J. 2020 September 18; 477(17): 3237–3252. doi:10.1042/BCJ20200480.

Source of ^{12}C in Calvin–Benson cycle intermediates and isoprene emitted from plant leaves fed with $^{13}CO_2$

Thomas D. Sharkey[1,2,3], **Alyssa L. Preiser**[1], **Sarathi M. Weraduwage**[1,3], **Linus Gog**[1,3]

[1]MSU-DOE Plant Research Laboratory and Department of Biochemistry and Molecular Biology, Michigan State University, East Lansing, MI 48824, U.S.A.

[2]Plant Resilience Institute, Michigan State University, East Lansing, MI 48824, U.S.A.

[3]Great Lakes Bioenergy Research Center, Michigan State University, East Lansing, MI 48824, U.S.A.

Abstract

Feeding $^{14}CO_2$ was crucial to uncovering the path of carbon in photosynthesis. Feeding $^{13}CO_2$ to photosynthesizing leaves emitting isoprene has been used to develop hypotheses about the sources of carbon for the methylerythritol 4-phosphate pathway, which makes the precursors for terpene synthesis in chloroplasts and bacteria. Both photosynthesis and isoprene studies found that products label very quickly (<10 min) up to 80–90% but the last 10–20% of labeling requires hours indicating a source of ^{12}C during photosynthesis and isoprene emission. Furthermore, studies with isoprene showed that the proportion of slow label could vary significantly. This was interpreted as a variable contribution of carbon from sources other than the Calvin–Benson cycle (CBC) feeding the methylerythritol 4-phosphate pathway. Here, we measured the degree of label in isoprene and photosynthetic metabolites 20 min after beginning to feed $^{13}CO_2$. Isoprene labeling was the same as labeling of photosynthesis intermediates. High temperature reduced the label in isoprene and photosynthesis intermediates by the same amount indicating no role for alternative carbon sources for isoprene. A model assuming glucose, fructose, and/or sucrose reenters the CBC as ribulose 5-phosphate through a cytosolic shunt involving glucose 6-phosphate dehydrogenase was consistent with the observations.

Introduction

The discovery of the path of carbon in photosynthesis was made possible by studies of the labeling of intermediates when $^{14}CO_2$ was fed to photosynthetic organisms [1]. While many observations were fully explained, some observations were not understood [1,2]. One of these observations is that when isotopes of carbon are fed to leaves as CO_2, the

Correspondence: Thomas D. Sharkey (tsharkey@msu.edu).

Author Contributions

T.D.S. conceived the idea, did the modeling, and had overall responsibility for writing the manuscript, A.L.P. and S.M.W. carried out the research and wrote parts of the manuscript, L.G. carried out the isoprene measurements reported in Figures 2 and 3.

Competing Interests

The authors declare that there are no competing interests associated with the manuscript.

intermediates of the Calvin–Benson cycle (CBC) label quickly (in 5–10 min) to between 80% and 90% but then do not label fully for hours [3–7].

A similar anomaly is found for labeling of isoprene, an early product of the methyl-D-erythritol 4-phosphate (MEP) pathway, emitted by many plants. This pathway occurs in the plastid and is the source of building blocks for many specialized terpenoid metabolites [8–12]. In the first step of the pathway, 1-deoxy-D-xylulose 5-phosphate (DXP) is synthesized from pyruvate and glyceraldehyde 3-phosphate (GAP) [13,14]. In later steps of the pathway, isopentenyl diphosphate (IDP) and dimethylallyl diphosphate (DMADP) are used as 5-carbon building blocks for terpenoids [15]. Isoprene is made from DMADP when isoprene synthase is present [16–18].

Isoprene is emitted by some, but not all, plants [19–24] and may help plants respond to ozone [25–27], singlet oxygen [28], and tolerate increases in temperature [19,29–34]. Isoprene emitted from trees also plays an important role in atmosphere chemistry [19,35–37].

One question in our understanding of the MEP pathway is the incomplete labeling in isoprene when fed $^{13}CO_2$. Isoprene will only label to ~80% within 20 min [38–42]. This was initially considered to reflect the labeling pattern in the CBC [38] but labeling of CBC intermediates and isoprene have never been measured for the same leaves.

It has been shown that labeling patterns in isoprene can vary. When eucalypts are heated from 30°C to 45°C, the proportion of unlabeled isoprene increases [43]. Similar results were shown with drought stress in poplar [44]. This variability in the degree of incomplete labeling has been considered to reflect carbon sources for the MEP pathway other than the CBC, especially pyruvate used by the MEP pathway [40,42,45–47]. However, it is unknown if CBC metabolites follow the same labeling pattern under these conditions. Here, we examined labeling patterns of the CBC and isoprene to determine if there are non-CBC carbon sources for the MEP pathway or if instead, isoprene labeling reflects changes in labeling of intermediates of the CBC, providing a window on metabolic changes in photosynthesis. We developed a model based on a cytosolic glucose 6-phosphate (G6P) shunt that can explain the observations of labeling of the CBC intermediates and isoprene and conclude that isoprene labeling accurately reflects CBC intermediates. Thus, isoprene provides a nondestructive window on labeling of the CBC intermediates.

Materials and methods

Plant material

Populus nigra × *maximowiczii* ‘NM6’ (a hybrid poplar) cuttings provided by Professor Kyung-Hwan Han of the Great Lakes Bioenergy Research Center (GLBRC) were planted in Suremix growing medium in 1 l pots. These pots were kept in a greenhouse and fertilized with 1/2-strength Hoagland’s solution [48] 3 days each week; plants were watered with deionized water the remaining 4 days of the week. The conditions in the greenhouse were recorded with the aid of HOBO data loggers (Onset Computer Corporation, MA). During the growth season the plants grew under a 16-h photoperiod, an average light intensity of

207 μmol m^{-2} s^{-1} during the middle 10 h of the photoperiod and average day/night temperatures of 25°C/18°C.

$^{13}CO_2$ labeling of poplar at steady state

Two-month-old poplar trees were used for the experiment. Two leaves, one for each temperature, from five trees were used. The 13th and 14th fully expanded leaf of each plant, counted from the apex of the stem, were used in the measurements. Pots with trees were brought to the laboratory and a leaf was inserted into the 11.46 cm^2 leaf chamber of the fast-kill instrument.

The fast-kill instrument was used as described in Schrader et al. [49]. A KL1500 quartz halogen lamp (Schott Glas, Mainz, Germany) was used to illuminate the top of the leaf chamber. The light intensity was set to 1000 μmol m^{-2} s^{-1}, measured with a LI-COR quantum sensor (LI-250A, LI-COR Biosciences, NE). The temperature inside the leaf chamber was controlled by a water bath circulating water in the aluminum block of the gas exchange chamber. A thermocouple inserted in the leaf chamber with the sensor touching the abaxial surface of the leaf was connected to a LI-6800 portable gas exchange system (LI-COR Biosciences, Lincoln, NE) that recorded the temperature in the leaf chamber. A custom chamber adapter (LI-6800–19) was used to connect the head of the LI-6800 to the leaf chamber of the fast kill to allow air flow between the LI-6800 and the leaf chamber.

Air containing 79% N_2 and 21% O_2, controlled by mass-flow controllers (Alicat Scientific, https://www.alicat.com), was humidified and then supplied to the LI-6800. Average water vapor content in the leaf chamber as read and recorded by the LI-6800 was 2.6 kPa. The Bev-A-Line tubing supplying gasses from the console to the head of the LI-6800 was interrupted close to the back of the LI-6800 head with a Swagelok T-joint to allow the supply of either unlabeled (99% $^{12}CO_2$) or labeled (99% $^{13}CO_2$, supplier — Sigma–Aldrich, MO) CO_2. The $^{13}CO_2$ was diluted with CO_2-free air to ~15% CO_2 in air. The supply of this $^{13}CO_2$ was controlled so that the concentration of CO_2 experienced by the leaf was the same regardless of which isotope was fed. A four-way ball valve before the point of injection of CO_2 to the T-joint allowed a rapid switch between either isotope of CO_2 to the gas stream. CO_2 was supplied by an external tank controlled by a 5 ml min^{-1} flow controller (Alicat Scientific, https://www.alicat.com) to bring the partial pressure of CO_2 in the air entering the leaf chamber to 41 Pa as measured by the sample IRGA. The entire chamber was switched over from $^{12}CO_2$ to ~90% $^{13}CO_2$ within 1 min.

First, the leaf was left to equilibrate for 90 min in the leaf chamber supplied with unlabeled CO_2 and at either 30°C or 40°C. During this period, photosynthesis and isoprene emission was measured simultaneously using the LI-6800 and a Fast Isoprene Sensor (FIS, Hills Scientific, CO), respectively. To measure isoprene, the exhaust air of the LI-6800 was directed to the FIS. Isoprene emission was averaged over 5 s intervals by the FIS. The operational basics of the FIS are described in Guenther and Hills [50]. The flow rates in the LI-6800 (500 μmol s^{-1}) and the FIS (280 μmol s^{-1}) allowed for 60% of the air stream from the leaf chamber to enter the FIS. After incubation for 90 min, the CO_2 supply was switched to $^{13}CO_2$ and held for 20 min. After 15 min of labeling, the exhaust port of the LI-6800 was immediately connected to the screw cap valve of a Tedlar gas sampling bag with

Thermogreen LB-2 Septa (Supelco, PA); by opening the screw cap valve, the gas efflux from the leaf chamber was collected in the Tedlar bag for 2 min, being careful not to induce a backpressure on the LI-COR. After 2 min the valve was closed and the Tedlar bag was labeled and stored. A 3.011 ppm isoprene standard was also collected in a Tedlar gas sampling bag.

At 20 min, the fast-kill mechanism was released causing liquid-nitrogen-cooled copper blocks to smash and freeze a leaf piece without interruption of the light source. Frozen leaves were collected in 2 ml microcentrifuge tubes and stored at −80°C for further analysis by mass spectrometry.

Additional justification for focusing on the 20 min time point

At 20 min, the fast phase of labeling is over. If the fast phase of labeling were to continue to 20 min, the labeling of CBC intermediates would be >99%. This is demonstrated with data taken from Szecowka et al. [5]. Ribulose 1,5-bisphosphate, 3-PGA, 2-PGA, and ADP glucose label essentially identically (Supplemental Figure S1A). The data for these four metabolites were averaged and subtracted from 100%. Plotting this data on a log scale reveals two lines representing the exponential decay of the fast phase and slow phase (Supplemental Figure S1B). The exponential decay rate determined by linear regression of the first three points was $-0.23\ min^{-1}$ while the slow phase exponential decay rate was $-0.014\ min^{-1}$. The lines cross at 12.7 min. A similar double exponential decay plot for isoprene labeling was published by Delwiche and Sharkey [38]. In that case, the fast phase exponential decay was $-0.17\ min^{-1}$ and the slow phase was $-0.08\ min^{-1}$. The lines cross at 6.9 min. Therefore, choosing 20 min for the time point to study ensures that fast labeling processes were finished but the system was still well within the second exponential decay phase and so our study was focused on processes in this second phase.

Metabolite extraction and mass spectrometry for metabolites

Phosphoglycerate (PGA), 6-phosphogluconate (6PG), ADP glucose, and UDP glucose were analyzed using methods modified from Lunn et al. [51]. We measured labeling in PGA instead of GAP, the immediate substrate for the MEP pathway. Levels of PGA are much higher than those of GAP and provide a more reliable signal. Frozen plant material was ground using a ball mill (Retsch, https://www.retsch.com) and suspended in 1.8 ml ice cold 30 : 70 chloroform : methanol. The mixture was incubated at −20°C for 2 h, vortexing every 0.5 h. Deionized water (1.5 ml) was added, samples were vortexed, and centrifuged at 22 000g for 10 min at 4°C. The aqueous fraction was collected and kept on ice. The non-aqueous fraction was re-extracted with an additional 1.5 ml deionized water and the second collected aqueous fraction was added to the first. Samples were frozen and freeze dried using a FreeZone Triad Freeze Dryer (Labconco, https://labconco.com). Dried samples were resuspended in 200 µl of 0.5 mM KOH and relative labeling of carbon in metabolites was measured using a coupled mass spectrometry.

Parameters for the detection of metabolites were optimized using 10 µM standards purchased from Sigma–Aldrich (https://www.sigmaaldrich.com) (Supplemental Table S1). LC/MS-MS was carried out at the Mass Spectrometry and Metabolomics Core of Michigan

State University (https://rtsf.natsci.msu.edu/mass-spectrometry/) on an Aquity TQD Tandem Quadrupole UPLC/MS/MS (Waters, https://www.waters.com) and was operated in electrospray negative ion mode with multiple reaction monitoring. The capillary voltage was 2.5 kV; the cone voltage, 2 V; the extractor voltage, 3 V. The source temperature was 130°C and the desolvation temperature was 350°C. Gas flow for the desolvation and cone was set to 700 and 40 l h^{-1}, respectively. MassLynx software and the Acquity UPLC Console were used to control the instrument. Samples were passed through a Dionex IonPac ATC-3 Trap Column, a Dionex IonPac AG11-HC Guard Column, and a Dionex IonPac AS11-HC Analytical Column (ThermoFisher Scientific, www.thermofisher.com) with a multi-step gradient, which was modified from Cocuron and Alonso [52] The flow rate was 0.35 ml min^{-1} with eluent A (0.5 mM KOH) and eluent B (75 mM KOH): 0–0.5 min, 100% A; 0.5–4 min, 100–95.2% A; 4–8 min, 95.2–87.3% A; 8–10 min, 87.3–73.8% A; 10–28 min, 73.8–33.5% A; 28–31 min, 33.6–0% A; 31–36 min, 0% A; 36–36.01 min, 0–100% A; 36.01–40 min, 100% A.

Mass spectrometry for isoprene

The analysis of isoprene samples was carried out using gas chromatography–mass spectrometry (GC/MS) at the Mass Spectrometry and Metabolomics Core of Michigan State University (https://rtsf.natsci.msu.edu/mass-spectrometry/). An Agilent 7010B Triple Quadrupole GC/MS system (Agilent, CA) was used. An EZ-Guard GC column was used (VF5 CP9013, Agilent, 30 m length, 10 m guard length, EZ Guard, 7 in cage, 0.25 mm inner diameter).

Isoprene collected in the Tedlar bag was sampled using a solid-phase microextraction (SPME) fused-silica fiber coated with Carboxen/Polydimethylsiloxane (Cat # 57318, Supelco, PA). After the oven had reached 230°C, and before being used for sampling, the needle end of the SPME fiber holder (Cat #577330-U, Supelco, PA) was placed in the heated zone of the GC injection port. The SPME fiber was carefully protruded into the GC injection port and locked into place in the exposed position. After conditioning the SPME fiber in the GC injection port for 20 min the fiber was retracted into the holder and removed from the GC injection port.

To facilitate the insertion of the SPME fiber into the Tedlar bag, a bag containing a gas sample was placed on the benchtop (with the screw cap facing upward) and the SPME fiber holder was positioned directly above it and held vertically and straight with the aid of a ring stand. Next, the Thermogreen LB-2 Septa of the Tedlar bag was pierced by the septum-piercing needle located at the end of the SPEME holder and the SPME fiber was inserted into the bag and allowed to adsorb analytes for 10 min. At the end of 10 min, the SPME fiber was carefully retracted from the Tedlar bag and immediately inserted into the injector port of the GC (as described previously) and was allowed to desorb for 2 min at 230°C. During desorption, isoprene was collected in a cryotrap cooled to −10°C with CO_2. Immediately after the 2 min desorption period, the AgilentQQQ/MassHunter program was started and run for 6.75 min. Isoprene was released from the cryotrap by rapid heating so that it entered the column as a very sharp band. Isoprene eluted at 1.4 min. At the end of the

program, the SPME fiber was retracted and the process was repeated with the rest of the gas samples.

Mass fragments of unlabeled isoprene (mass-to-charge ratio [m/z] 67, 68), and its isotopologues containing one to five ^{13}C carbons (up to $m/z = 73$) were measured by the mass spectrometer of the Agilent 7010B Triple Quadrupole GC/MS system. Quality analysis and the mass spectra were generated by the AgilentQQQ/MassHunter program.

Data analysis

The mass spectra obtained from the ^{13}C labeled CBC metabolites were analyzed using TargetLynx Application Manager, an option with Waters MassLynx™ Software, (Waters Corporation, MA). The ion ratios and peak areas automatically generated by TargetLynx were manually reviewed to optimize peak integration. The final outputs included the reaction time, peak area, peak quality as indicated by the signal to noise ratio. The peak areas represent the abundance of the mass fragments of interest.

During chemical ionization, some isoprene loses a proton such that the most abundant ion in the mass spectrum is the M − 1 ion but there also is a significant amount of the M + 0 ion. Therefore, the mass spectrometer data were deconvoluted to separate the contribution of the two ions of each isotopologue. The isoprene isotopologues (^{i}I, where i is the molecular mass, e.g. with no ^{13}C $i = 68$) were computed from the ion counts at different mass-to-charge readings (^{j}M, where j is the m/z for the ith ion). Therefore, the total amount of the isotopologue with no ^{13}C would be

$$^{68}I = {}^{67}M + {}^{68}M \tag{1}$$

The proportion of ions at M − 1, α, can be estimated as follows using the mass spectrum of isoprene from an unlabeled leaf:

$$\alpha = \frac{^{67}M}{\left(^{67}M + {}^{68}M - 0.055 \cdot \frac{^{67}M}{\alpha}\right)} \tag{2}$$

Because eqn 2 is not fully solved for α it must be solved iteratively. The presumed natural abundance of ^{13}C in isoprene (1.1% of carbons) is accounted for by the term $^{68}M - 0.055 \cdot {}^{67}M/\alpha$. Data obtained in this study yielded $\alpha = 0.62$. Each isotopologue was computed as

$$^{i}I = (^{j}M - {}^{i-1}I \cdot (1 - \alpha))/\alpha \tag{3}$$

In the case of ^{68}I, there is no $i - 1$ isotopologue so the equation simplifies to

$$^{68}I = {}^{67}M/\alpha \tag{4}$$

Model development

A model was made to explore whether cytosolic oxidative pentose phosphate pathway activity, the cytosolic G6P shunt, and hexokinase and fructokinase could allow unlabeled

carbon to enter the CBC and so account for the lack of full labeling and the variation in labeling seen in isoprene studies (Figure 1). The model has velocities (v), rates in terms of carbon atoms, adjusted when necessary to account for the number of carbon atoms per molecule and relative to net assimilation, and ratios (R), the ratio of carbon 13 to carbon 12 in the molecule. The model is a snapshot in time after 20 min of labeling so that short term reactions are saturated and focus is on the long-term lack of labeling.

Pools joined by reversible reactions are assumed to be in isotopic equilibrium and collapsed to a single pool. The CBC intermediates as well as ADPG are considered one pool based on labeling patterns reported here and in several comprehensive studies [5–7]. Likewise, the hexose phosphates in the cytosol are considered to be in isotopic equilibrium. This is may not be true in the plastid but this is ignored since ADPG has a similar degree of label as PGA and RuBP so there is no evidence of a strong variation in labeling from F6P to G6P in the chloroplast. When there are two inputs into a pool, the ratio in that pool will be the velocity-weighted average of the precursor ratios.

This modeling was developed to ask two things (1) for a given ratio of isotopes in the CBC (R_3), assuming all of the unlabeled carbon is coming from a cytosolic G6P shunt, what degree of labeling is expected in the cytosolic carbon as assessed by the label in UDPG? and (2) what rate of the cytosolic G6P shunt is needed to account for the lack of complete labeling of the CBC? The model approximates mass balance by assuming some sucrose is added to the large sucrose pool and the large sucrose pool undergoes some breakdown by invertase or sucrose synthase. The free hexoses can then reenter the active carbon pool by hexokinase and fructokinase (Figure 1). Since the leaf glucose-6-phosphate transporter (GPT2) is normally not expressed in photosynthetic tissue [53,54] it is necessary that the hexose phosphates be converted to pentose phosphates for entry into chloroplasts on the xylulose phosphate transporter (XPT) [55,56]. It is assumed that the flux through sucrose, glucose, and fructose is small relative to their pool sizes. Two scenarios are modeled, one assuming negligible amounts of label in glucose, fructose, and sucrose pools and one assuming those pools are labeled to 22% at 20 min. In sucrose synthesis during photosynthesis, G6P is metabolized to glucose 1-phosphate and then UDPG. In this model, some part of the cytosolic G6P may be acted on by G6PDH and eventually reenter the CBC as either Ru5P or refixed CO_2 diluting the label in the CBC. The oxidative pentose phosphate pathway should be active, at least to some degree in the light [57].

The initial ratio, R_1 is assumed to be 99% since most $^{13}CO_2$ sources have this abundance ratio. This ratio is diluted by refixed carbon from the cytosolic G6P shunt. We assumed that because of stomatal and mesophyll resistance to CO_2 diffusion, approximately half of the CO_2 released in the G6P shunt would be refixed and half would escape to the atmosphere. Although this could be an underestimation [58] the model output was not very sensitive to variations in this assumption. To have net assimilation = 1,

$$v_1 = 1 \tag{5}$$

and

$$R_2 = (v_1\ R_1 + 0.5 \cdot v_8 \cdot R_6)/(v_1 + 0.5 \cdot v_8) \quad (6)$$

This CO_2 enters the CBC by fixation by rubisco and the CBC also receives Ru5P from the G6P shunt. Therefore, the ratio of 13–12 carbon in the CBC is

$$v_2 = 1 + 0.5 \cdot v_8 \quad (7)$$

$$R_3 = (v_2\ R_2 + v_8 \cdot 5 \cdot R_6)/(v_2 + 5v_8) \quad (8)$$

The ratio R_3 is assumed to be the ratio for all molecules in the CBC and also ADPG and will be reported as ADPG. The majority of effects of photorespiration on labeling should be finished within a few minutes of beginning to label with $^{13}CO_2$ [5] and so photorespiration is ignored here. There are pools of glycine, serine, and glycerate that do not rapidly label which could contribute if they exchange slowly with the active pools, but these potential effects are ignored in this treatment and would not explain the reduced degree of label in UDPG. Karl et al. [40] found that low oxygen decreased the degree of label rather than increasing it as would be expected if the source of ^{12}C were serine or glycine from photorespiration. Equation 8 shows how the G6P shunt can have a significant effect on labeling since five carbons enter the CBC as Ru5P for each reaction of G6P dehydrogenase of the G6P Shunt.

In the model, label in the CBC will be affected by the label in the cytosolic hexose-phosphate pool, which is dependent on label in the CBC. As a result, the model must be solved by iteration. An initial guess of the value of R_6 is used to calculate the other values in the model. These are then used to calculate R_6.

$$R_6 = (v_4 R_3 + 6 \cdot v_8 R_5)/(v_4 + 6 \cdot v_8) \quad (9)$$

The guess is then updated and used in eqn 8 again until the guess and calculated R_6 are equal (using the Solver add-in of Excel). The model was run in Excel assuming the cytosolic G6P shunt varied over a range from zero to 0.2 times the net assimilation rate. The excel file used is supplied as supplemental material.

Results

Steady-state ^{13}C labeling in central carbon metabolism and isoprene

We measured isoprene labeling and compared that with labeling of representative metabolites of the CBC and 6PG of the G6P shunts (found in both the plastid and cytosol). 3-phosphoglycerate (PGA), isoprene, fructose 6-phosphate (F6P) plus G6P (not separated), and ribose 5-phosphate (R5P) all labeled to between 80% and 85% (Figure 2). Ribulose 1,5-bisphosphate (RuBP) labeled to just 76% and was statistically significantly lower than PGA (two-tailed *t*-test with unequal variance, $F = 11.04$, df 4, $P = 0.007$). Even less label was found in 6PG.

A certain amount of isoprene (6%) remained fully unlabeled while singly labeled isoprene was just 2% of the total (Figure 3). We hypothesized that this could result from the retrograde signal metabolite methyl erythritol 2,4-cyclophosphate (MEcDP) exchanging slowly between the chloroplast and cytosol and nucleus [59–61] with the unlabeled MEcDP, therefore, diluting the label in isoprene. This explanation is consistent with observations of Karl et al. [40] and Loreto et al. [62] that feeding fosmidomycin reduced emission of labeled isoprene much more than the emission of the unlabeled isotopologue. If the data are corrected for this effect by assuming that all unlabeled isoprene came from MEcDP and so should be excluded from the analysis, the degree of label of carbon entering the MEP pathway increased from 82.4 ± 2.4% to 87.7 ± 2.7% (mean ± SD, $n = 5$). The degree of label of carbon entering the MEP pathway, therefore, probably lies somewhere between these two numbers but given the singly labeled isoprene was one third less than the unlabeled isoprene, the correct ratio for carbon coming from the CBC is likely closer to the upper end of this range and can be compared with the degree of label of PGA at 85.7 ± 2.0%.

The metabolite that had the lowest degree of label was 6PG. This metabolite is the result of the activity of G6P dehydrogenase (G6PDH) and so we expected G6P to be similar to 6PG labeling. We did not see that in this case, but our measurement included both G6P and F6P in both the chloroplast and cytosol. To rectify this problem, in subsequent experiments we measured ADP glucose (ADPG) to assess the label in G6P in the chloroplast and UDP glucose (UDPG) to assess the label in G6P in the cytosol (Figure 1).

We next tested whether stress effects that cause a reduction in the degree of labeling of isoprene also changed the degree of labeling in CBC intermediates. We chose temperature as reported by Guidolotti et al. [43] to decrease label in isoprene. Photosynthesis was significantly inhibited while isoprene emission was significantly stimulated by increasing leaf temperature from 30°C to 40°C (Table 1). The Q_{10} for isoprene emission was well in excess of 2. At 30°C, we found that 93.2 ± 1.7% of the carbon in PGA labeled with ^{13}C while 88.7 ± 1.4% of isoprene carbon was ^{13}C (Figure 4) (this value is corrected for the fully unlabeled isoprene thought to arise from a slow back diffusion of MEcDP, without this correction the value was 84.0 ± 1.7%.) The label in the glucose moiety of ADPG was labeled to the same degree as PGA and isoprene, suggesting that all CBC intermediates and precursors for isoprene synthesis were equally labeled.

In the cytosol, UDPG was significantly less labeled than the chloroplastic compounds (two-tailed Student's *t*-test of the difference in the degree of label between isoprene and UDPG, $P = 0.004$) (Figure 4). Assuming UDPG reflects the G6P in the cytosol, and if 6PG is made by a cytosolic G6P shunt through G6PDH then 6PG should have the same degree of labeling as UDPG. At 30°C the difference in labeling of UDPG and 6PG was not statistically significant (two-tailed Student's *t*-test $P = 0.105$).

At 40°C there was much less label in isoprene than at 30°C (Figure 4). However, rather than indicating alternative sources of carbon for the MEP pathway, the decline in label in isoprene accurately reflected a decline in label in PGA and ADPG (two-tailed Student's *t*-test of the difference between isoprene and PGA labeling was $P = 0.365$). The high temperature caused a significant drop in the degree of label in UDPG (two-tailed Student's *t*-

test $P = 0.005$). Unlike at 30°C, the label in 6PG was significantly higher than in UDPG (two-tailed Student's *t*-test $P = 0.0002$). The amount of completely unlabeled isoprene isotopologue was not different between the two treatments (Figure 5). A more complete dataset of all isotopologues for this experiment is provided in Supplemental Table S2. This dataset shows that the pattern of isotopologue abundance for ADPG and isoprene and for UDPG and 6-PG were similar at 30°C but the similarity between UDPG and 6-PG broke down at 40°C.

Modeling

Three scenarios were run, one assuming that the carbon coming into the hexose-phosphate pool in the cytosol had natural abundance degree of labeling (6.6%), and a second where it was assumed that this carbon had become labeled to 22%, the value reported for sucrose at 20 min by Szecowka et al. [5]. This is a high value because glucose and fructose labeled more slowly than sucrose and were much less than 22% even at 1 h [5]. For the above two scenarios, the rate of sucrose synthesis was set to 30% of net assimilation. A third run with ^{13}C content of glucose/fructose set to 6.6% and carbon partitioning to sucrose set to 10% was run to test the model for sensitivity to this assumption (possibly reflecting a shift in the metabolism under stressful conditions). The effect of the G6P shunt on degree of label in ADPG and UDPG are shown as lines in Figure 6. The data points in Figure 6 are the data for ADPG and UDPG in Figure 4. The degree of label in ADPG was used to select a position along the *x*-axis to place the data for both ADPG and UDPG at both 30 and 40°C (Figure 6). The model shows that hexokinase and fructokinase plus a cytosolic G6P shunt can explain the lack of full labeling in the CBC. The data fit the scenario of natural abundance labeled carbon coming into the cytosolic hexose pool as a result of hexokinase and/or fructokinase (Figure 1) but the difference in assuming 22% label in this pool (dashed lines) is not great. The experimental data are plotted at a G6P shunt rate of 0.05 times the rate of net CO_2 fixation at 30°C and 0.16 times the rate of net CO_2 fixation at 40°C.

Discussion

Lack of complete labeling of the CBC and isoprene

It has been shown that PGA and isoprene remain partially unlabeled when fed $^{13}CO_2$ or $^{14}CO_2$ [5–7,38–40,63,64]. Although the first report of incomplete labeling of isoprene pointed out the connection between incomplete labeling of the CBC and isoprene [38], most reports of isoprene labeling have interpreted incomplete labeling in isoprene as an indication of carbon sources other than the CBC, often proposing an alternative source for pyruvate, typically by glycolysis of old carbon [42,45]. In other words, label in isoprene was the result of fully labeled GAP and a variable amount of unlabeled pyruvate. By measuring isoprene labeling and labeling in PGA and other plastidial metabolites we now show that it is possible to account for the labeling patterns of isoprene assuming all carbon for isoprene (and thus the MEP pathway) come only from the CBC. Because GAP labeling is similar to isoprene and changes in isoprene labeling match changes in GAP labeling, variable pyruvate labeling adding to fully labeled GAP is not responsible for variable isoprene labeling.

Many metabolites had more M0 than M1 isotopologues. This is consistent with a source of carbon skeletons that is completely unlabeled. Ma et al. [6] attribute this to a small pool that is isolated from metabolism but we suggest it represents a flux of carbon from unlabeled free glucose, through the cytosolic G6P shunt, and back to the CBC by way of the xylulose 5-phosphate/phosphate transporter [55,56]. If completely unlabeled pentose phosphates entered the CBC at a rate of 2% of carboxylation, the maximum degree of labeling would be limited to 90% (2% times five unlabeled carbons). After 20 min of labeling this may better explain the lack of complete labeling than the position-specific labeling of CBC reactions [65].

There is an additional small flux of completely unlabeled carbon into isoprene at 30°C (Figures 3 and 5 and [66]) that is not sensitive to fosmidomycin [40]. The rate of this input was similar at different temperatures and did not account for the changes in the degree of label caused by high temperature. We hypothesize that this results from a slow equilibration of the MeCDP pool between the chloroplast and other compartments of the cell. From data in [66] it appears that whole-cell MEcDP has a slightly higher degree of totally unlabeled isotopologues than in isoprene, consistent with this hypothesis.

To account for the data, the G6P shunt should have a rate of 5% of net photosynthesis at 30°C and 18% at 40°C. The net rate of photosynthesis fell from 15.8 ± 3.1 (mean ± SD, n = 5) to 6.6 ± 1.7. The decline in photosynthetic rate by itself (15.8/6.6 = 2.39) would have changed the relative rate of the G6P shunt to 12% (5% × 2.39 = 12%). In other words, about one half of the apparent increase in G6P shunt rate at high temperature resulted from the decline in photosynthetic rate, the rest from a stimulation of the shunt.

One observation made to support alternative sources of pyruvate is that labeling of the methyl vinyl fragment of isoprene (carbons 3, 4, and 5 coming from carbons 2 and 3 of pyruvate and carbon 3 of GAP) labels more slowly than does the whole isoprene molecule [42]. However, the GAP and pyruvate derived from the CBC can have position-specific variations in labeling. The methyl vinyl fragment of isoprene would come from positions two and three of PGA and these should label much more slowly than position one of GAP [2,67], which is present only in the whole isoprene molecule, not the methyl vinyl fragment. The uneven distribution of label among positions can be seen in sucrose even after 15 min of labeling [68]. Thus, the difference in labeling of the methyl vinyl fragment could simply reflect position-specific labeling arising in the CBC [1].

No role for glycolysis—The presumed non-CBC source of unlabeled carbon in many reports is pyruvate from glycolysis [40,42]. However, photosynthesis and glycolysis cannot occur simultaneously because fructose bisphosphatase and phosphofructokinase comprise a futile cycle. To prevent futile cycling, fructose bisphosphatase is very sensitive to fructose 2,6-bisphosphate while phosphofructokinase activity depends on it [69]. In the dark there is fructose 2,6-bisphosphate present, allowing glycolysis to proceed, but it is dephosphorylated to F6P in the light, switching cytosolic metabolism from glycolysis to gluconeogenesis [70]. Labeling studies also rule out an alternative, unlabeled source of pyruvate in photosynthesizing leaves. In the studies of Szecowka et al. [5] and Ma et al. [6] phospho*enol*pyruvate or 2-phosphoglyceric acid (present only in the cytosol) labeled to the

same degree as CBC intermediates showing that pyruvate comes from the CBC during photosynthesis.

Little role for photorespiration—There is a relatively large pool of serine that labels more slowly than CBC intermediates. The nature of this pool, for example, its cellular location and turnover, are not known. It is possible that some unlabeled serine is returned to the CBC, thus diluting the CBC intermediates. However, using pool size and photosynthetic rate in Szecowka et al. [5] it can be calculated that serine is a much smaller source of unlabeled carbon than are the hexose (plus sucrose) pools (Table 2). Whether the serine contribution would increase at high temperature is unknown, but it is likely still much less than the shunts.

A similar analysis indicates that among organic acids, only glutamate could provide a significant source of unlabeled carbon skeletons (Table 2) but it is not clear how glutamate would be converted to a compound that could rejoin the CBC.

The G6P shunts return carbon to the CBC

The cytosolic G6P shunt explains how carbon from the cytosol can reenter the CBC. The shunt has been proposed as a mechanism for stabilizing photosynthesis, especially in a rapidly fluctuating light environment [71]. In response to stress and in CBC enzyme loss-of-function mutants, a plastidial shunt also occurs. The plastidial shunt may be regulated by stromal G6P concentration and/or H_2O_2 [57]. Both the plastidial and cytosolic shunts may lead to high cyclic electron flow rates [72].

The cytosolic shunt can return unlabeled carbon to the CBC as a result of hexokinase action on glucose and fructokinase action on fructose [73]. Hexose phosphates generally are not transported across chloroplast membranes of photosynthesizing leaves [53,54], but after conversion to ribulose 5-phosphate and isomerization to xylulose 5-phosphate this carbon can reenter the chloroplast and CBC on the XPT, which can transport both xylulose and ribulose 5-phosphate [55,56]. The activity of cytosolic hexokinase may cause sugar signaling that could adjust photosynthetic activity and co-ordinate photosynthesis with other physiological processes in plants [74]. The degree to which glucose and fructose are made from sucrose and the enzyme involved (invertase versus sucrose synthase) is not known.

Distinguishing between the plastidial shunt and the cytosolic shunt—In the model presented here, it is assumed that at 30°C all of the shunt activity is cytosolic, and this is why 6PG has a degree of label indistinguishable from UDPG, assumed to be identical with G6P in the cytosol.

At 40°C the labeling is consistent with an increased cytosolic G6P shunt relative to 30°C. UDPG label indicates that cytosolic hexose phosphates, CBC intermediates, and ADPG all have less label at 40°C. However, 6PG is more heavily labeled than at 30°C and at 40°C more heavily labeled than UDPG. This is consistent with high temperature stimulating the plastidial G6P shunt. Because the 6PG label (64%) is closer to ADPG (73%) than to UDPG (41%) it is likely that the plastidial shunt is going faster than the cytosolic shunt at high temperature. Making the assumption that pools sizes are not a major factor in labeling

kinetics of 6PG it can be estimated that the plastidial shunt should be going 2.5 times faster than the cytosolic shunt in order to get the labeling pattern seen in 6PG. We do not think this is a result of changes in gene expression or protein synthesis but rather that stress stimulates the activity of plastidial G6PDH, which is normally not active in the light. We have recently shown that plastidial G6PDH can be activated in the light, for example by the accumulation of H_2O_2 [57], causing the plastidial shunt. However, this is not a source of ^{12}C since carbon going through the plastidial shunt will start with a degree of label the same as what gets reinjected into the CBC. Previous hypotheses that starch turnover might cause the plastidial shunt to inject unlabeled carbon into the CBC [1,75] is ruled out by labeling patterns of ADPG and UDPG. Other studies found that maltose labels slowly ([5], Supplemental Table S2) but we showed that during the day most maltose present in leaves is the metabolically inert α anomer as opposed to the metabolically active β anomer present at night [76].

Energetics—Carboxylation of RuBP and subsequent reactions can result in one G6P. If that G6P enters the shunt, a cycle is formed that consumes and releases one CO_2, consumes two NADPH in PGA reduction and produces two NADPH in the G6P shunt, and consumes three ATP — one to convert Ru5P to RuBP and two during the conversion of PGA to GAP. Thus, the cost of the G6P shunt is three ATP. At a shunt rate of 0.05 times A, the total ATP demand would increase by 0.15 per net CO_2 fixed and increase the required ATP/NADPH ratio from 3/2 to 3.15/2, similar to or slightly less than the effect of photorespiration on the ATP/NADPH ratio.

The cytosolic shunt is modeled to be going faster at 40°C, increasing ATP usage significantly. Assuming the cytosolic shunt at 16% of A, the plastidial shunt at 2.5 times that rate, and three ATP used in each occurrence of the shunt gives $(0.16 + 2.5 \times 0.16) \times 3 = 1.68$ ATP on top of the three ATP used per CO_2 assimilated. The ATP to NADPH ratio, in that case, would be 4.68/2. Linear electron flow from water to NADPH is believed to produce 2.57 ATP per two NADPH resulting in an ATP deficit. At high temperature, with high rates of G6P shunts, both in the plastid and cytosol, the ATP deficit would be 2.12 compared with 0.58 for photosynthesis plus 5% G6P shunt rate and compared with 0.43 for CO_2 fixation in the absence of any shunt or photorespiration. The large ATP deficit at high temperature would require a significant rate of cyclic electron flow and it is well-known that high temperature stimulates cyclic electron flow [77–81]. The mechanism of this stimulation could involve an accumulation of H_2O_2, which is known to stimulate cyclic electron flow [82] and the plastidial G6PDH [57].

Isoprene as a window on labeling of the CBC

An understanding of the carbon source for the MEP pathway also provides a unique tool to examine the source of the slow-to-label carbon pool in the CBC. The amount of label in isoprene is a direct reflection of the amount of label in the CBC and can be used as a non-invasive measurement of the labeling status of PGA.

Previous reports of the variability of the degree of label of isoprene [40,42,43,62] can be reinterpreted as changes in the relative degree of label in the CBC and likely variation in the relative rate of the G6P shunt either by changes in the rate of the shunt or altered rates of

CO_2 assimilation. The measurements cited above indicate that several types of stress can increase the rate of the G6P shunt relative to the rate of net assimilation.

Model plants engineered to emit isoprene, like *Arabidopsis thaliana*, can be manipulated to test hypotheses for the source of the slow-to-label pool. Samples can easily be collected non-destructively and analyzed with isoprene capture and subsequent mass spectrometry. Samples collected this way do not have complications with sample collection and degradation like CBC metabolites.

Conclusion

Contrary to previous thought, we have shown that the CBC is the only source of carbon for the MEP pathway and isoprene synthesis. Additionally, we have provided a novel tool for analyzing labeling patterns of the CBC.

Supplementary Material

Refer to Web version on PubMed Central for supplementary material.

Acknowledgements

We are grateful to Jim Klug and Cody Keilen (Growth Chamber Facility), along with Dr. Tony Schilmiller, Lijun Chen, and Dr. Casey Johnny (Research Technology Support Facility - Mass Spectrometry and Metabolomics Core) of Michigan State University for their expertize and assistance. We thank Jacob Sylvestor (Department of Integrative Biology, Michigan State University) for assisting with the growth and maintenance of poplar plants, and Dr. Sean Weise and all members of the Sharkey laboratory for their support.

Funding

This research was funded by the U.S. Department of Energy Grant DE-FG02-91ER2002 (T.D.S., A.L.P.) and by the Great Lakes Bioenergy Research Center, U.S. Department of Energy, Office of Science, Office of Biological and Environmental Research under award number DE-SC0018409 (S.M.W., L.G.). The U.S. National Science Foundation supported publication of this work. Michigan AgBioResearch provided partial salary support for T.D.S.

Abbreviations

6PG	6-phosphogluconate
DMADP	dimethylallyl diphosphate
FIS	Fast Isoprene Sensor
G6P	glucose 6-phosphate
GAP	glyceraldehyde 3-phosphate
MEcDP	methyl erythritol 2,4-cyclophosphate
MEP	methyl-D-erythritol 4-phosphate
PGA	phosphoglycerate
SPME	solid phase microextraction

XPT	xylulose phosphate transporter

References

1. Sharkey TD (2019) Discovery of the canonical Calvin–Benson cycle. Photosyn. Res 140, 235–252 10.1007/s11120-018-0600-2
2. Ebenhöh O and Spelberg S (2018) The importance of the photosynthetic Gibbs effect in the elucidation of the Calvin–Benson–Bassham cycle. Biochem. Soc. Trans 46, 131 10.1042/BST20170245 [PubMed: 29305411]
3. McVetty PBE and Canvin DT (1981) Inhibition of photosynthesis by low oxygen concentrations. Can. J. Bot 59, 721–725 10.1139/b81-102
4. Mahon JD, Fock H and Canvin DT (1974) Changes in specific radioactivity of sunflower leaf metabolites during photosynthesis in $^{14}CO_2$ and $^{14}CO_2$ at three concentrations of CO_2. Planta 120, 245–254 10.1007/BF00390292 [PubMed: 24442699]
5. Szecowka M, Heise R, Tohge T, Nunes-Nesi A, Vosloh D, Huege J et al. (2013) Metabolic fluxes in an illuminated Arabidopsis rosette. Plant Cell 25, 694–714 10.1105/tpc.112.106989 [PubMed: 23444331]
6. Ma F, Jazmin LJ, Young JD and Allen DK (2014) Isotopically nonstationary ^{13}C flux analysis of changes in Arabidopsis thaliana leaf metabolism due to high light acclimation. Proc. Nat. Acad. Sci. U.S.A 111, 16967–16972 10.1073/pnas.1319485111
7. Hasunuma T, Harada K, Miyazawa S-I, Kondo A, Fukusaki E and Miyake C (2010) Metabolic turnover analysis by a combination of in vivo ^{13}C-labelling from $^{13}CO_2$ and metabolic profiling with CE-MS/MS reveals rate-limiting steps of the C_3 photosynthetic pathway in Nicotiana tabacum leaves. J. Exp. Bot 61, 1041–1051 10.1093/jxb/erp374 [PubMed: 20026474]
8. Arigoni D, Sagner S, Latzel C, Eisenreich W, Bacher A and Zenk MH (1997) Terpenoid biosynthesis from 1-deoxy-D-xylulose in higher plants by intramolecular skeletal rearrangement. Proc. Nat. Acad. Sci. U.S.A 94, 10600–10605 10.1073/pnas.94.20.10600
9. Lichtenthaler HK, Rohmer M and Schwender J (1997) Two independent biochemical pathways for isopentenyl diphosphate and isoprenoid biosynthesis in higher plants. Physiol. Plant 101, 643–652 10.1111/j.1399-3054.1997.tb01049.x
10. Lichtenthaler HK, Schwender J, Disch A and Rohmer M (1997) Biosynthesis of isoprenoids in higher plant chloroplasts proceeds via a mevalonate-independent pathway. FEBS Lett. 400, 271–274 10.1016/S0014-5793(96)01404-4 [PubMed: 9009212]
11. Schwender J, Zeidler J, Gröner R, Müller C, Focke M, Braun S et al. (1997) Incorporation of 1-deoxy-D-xylulose into isoprene and phytol by higher plants and algae. FEBS Lett. 414, 129–134 10.1016/S0014-5793(97)01002-8 [PubMed: 9305746]
12. Zeidler JG, Lichtenthaler HK, May HU and Lichtenthaler FW (1997) Is isoprene emitted by plants synthesized via the novel isopentenyl pyrophosphate pathway? Z. Naturforsch 52, 15–23 10.1515/znc-1997-1-204
13. Rohmer M, Seemann M, Horbach S, Bringer-Meyer S and Sahm H (1996) Glyceraldehyde 3-phosphate and pyruvate as precursors of isoprenic units in an alternative non-mevalonate pathway for terpenoid biosynthesis. J. Am. Chem. Soc 118, 2564–2566 10.1021/ja9538344
14. Estévez JM, Cantero A, Romero C, Kawaide H, JimQnez LF, Kuzuyama T et al. (2000) Analysis of the expression of CLA1, a gene that encodes the 1-deoxyxylulose 5-phosphate synthase of the 2-C -methyl-D-erythritol-4-phosphate pathway in Arabidopsis. Plant Physiol. 124, 95–103 10.1104/pp.124.1.95 [PubMed: 10982425]
15. Buchanan BB, Gruissem W and Jones RL (2015) Biochemistry & Molecular Biology of Plants. Chicester, Wiley Blackwell, West Sussex
16. Silver GM and Fall R (1991) Enzymatic synthesis of isoprene from dimethylallyl diphosphate in aspen leaf extracts. Plant Physiol. 97, 1588–1591 10.1104/pp.97.4.1588 [PubMed: 16668590]
17. Silver GM and Fall R (1995) Characterization of aspen isoprene synthase, an enzyme responsible for leaf isoprene emission to the atmosphere. J. Biol. Chem 270, 13010–13016 10.1074/jbc.270.22.13010 [PubMed: 7768893]

18. Miller B, Oschinski C and Zimmer W (2001) First isolation of an isoprene synthase gene from poplar and successful expression of the gene in Escherichia coli. Planta 213, 483–487 10.1007/s004250100557 [PubMed: 11506373]
19. Sharkey TD, Wiberley AE and Donohue AR (2008) Isoprene emission from plants: Why and how. Ann. Bot 101, 5–18 10.1093/aob/mcm240 [PubMed: 17921528]
20. Harley PC, Monson RK and Lerdau MT (1999) Ecological and evolutionary aspects of isoprene emission from plants. Oecologia 118, 109–123 10.1007/s004420050709 [PubMed: 28307685]
21. Delfine S, Alvino A, Zacchini M and Loreto F (1998) Consequences of salt stress on conductance to CO_2 diffusion, Rubisco characteristics and anatomy of spinach leaves. Aust. J. Plant Physiol 25, 395–402 10.1071/PP97161
22. Delfine S, Tognetti R, Loreto F and Alvino A (2002) Physiological and growth responses to water stress in field-grown bell pepper (*Capsicum annuum* L. J. Hort. Sci. Biotech 77, 697–704 10.1080/14620316.2002.11511559
23. Harley P, Vasconcellos P, Vierling L, Pinheiro CCDS, Greenberg J, Guenther A et al. (2004) Variation in potential for isoprene emissions among Neotropical forest sites. Global Change Biol. 10, 630–650 10.1111/j.1529-8817.2003.00760.x
24. Hanson DT, Swanson S, Graham LE and Sharkey TD (1999) Evolutionary significance of isoprene emission from mosses. Am. J. Bot 86, 634–639 10.2307/2656571 [PubMed: 10330065]
25. Vickers CE, Possell M, Cojocariu CI, Velikova VB, Laothawornkitkul J, Ryan A et al. (2009) Isoprene synthesis protects transgenic tobacco plants from oxidative stress. Plant Cell Environ. 32, 520–531 10.1111/j.1365-3040.2009.01946.x [PubMed: 19183288]
26. Loreto F and Velikova V (2001) Isoprene produced by leaves protects the photosynthetic apparatus against ozone damage, quenches ozone products, and reduces lipid peroxidation of cellular membranes. Plant Physiol. 127, 1781–1787 10.1104/pp.010497 [PubMed: 11743121]
27. Loreto F, Mannozzi M, Maris C, Nascetti P, Ferranti F and Pasqualini S (2001) Ozone quenching properties of isoprene and its antioxidant role in leaves. Plant Physiol. 126, 993–1000 10.1104/pp.126.3.993 [PubMed: 11457950]
28. Affek HP and Yakir D (2002) Protection by isoprene against singlet oxygen in leaves. Plant Physiol. 129, 269–277 10.1104/pp.010909 [PubMed: 12011357]
29. Pollastri S, Tsonev T and Loreto F (2014) Isoprene improves photochemical efficiency and enhances heat dissipation in plants at physiological temperatures. J. Exp. Bot 65, 1565–1570 10.1093/jxb/eru033 [PubMed: 24676032]
30. Velikova V, Varkonyi Z, Szabo M, Maslenkova L, Nogues I, Kovacs L et al. (2011) Increased thermostability of thylakoid membranes in isoprene-emitting leaves probed with three biophysical techniques. Plant Physiol. 157, 905–916 10.1104/pp.111.182519 [PubMed: 21807886]
31. Sasaki K, Saito T, Lamsa M, Oksman-Caldentey KM, Suzuki M, Ohyama K et al. (2007) Plants utilize isoprene emission as a thermotolerance mechanism. Plant Cell Physiol. 48, 1254–1262 10.1093/pcp/pcm104 [PubMed: 17711876]
32. Velikova V and Loreto F (2005) On the relationship between isoprene emission and thermotolerance in Phragmites australis leaves exposed to high temperatures and during the recovery from a heat stress. Plant Cell Environ. 28, 318–327 10.1111/j.1365-3040.2004.01314.x
33. Singsaas EL, Lerdau M, Winter K and Sharkey TD (1997) Isoprene increases thermotolerance of isoprene-emitting species. Plant Physiol. 115, 1413–1420 10.1104/pp.115.4.1413 [PubMed: 12223874]
34. Behnke K, Ehlting B, Teuber M, Bauerfeind M, Louis S, Hansch R et al. (2007) Transgenic, non-isoprene emitting poplars don't like it hot. Plant J. 51, 485–499 10.1111/j.1365-313X.2007.03157.x [PubMed: 17587235]
35. Guenther A, Karl T, Harley P, Wiedinmyer C, Palmer PI and Geron C (2006) Estimates of global terrestrial isoprene emissions using MEGAN (Model of Emissions of Gases and Aerosols from Nature). Atmos. Chem. Phys 6, 3181–3210 10.5194/acp-6-3181-2006
36. Su L, Patton EG, Vilà-Guerau de Arellano J, Guenther AB, Kaser L, Yuan B et al. (2016) Understanding isoprene photooxidation using observations and modeling over a subtropical forest in the southeastern US. Atmos. Chem. Phys 16, 7725–7741 10.5194/acp-16-7725-2016

37. Xiong F, McAvey KM, Pratt KA, Groff CJ, Hostetler MA, Lipton MA et al. (2015) Observation of isoprene hydroxynitrates in the southeastern United States and implications for the fate of NOx. Atmos. Chem. Phys 15, 11257–11272 10.5194/acp-15-11257-2015
38. Delwiche CF and Sharkey TD (1993) Rapid appearance of ^{13}C in biogenic isoprene when $^{13}CO_2$ is fed to intact leaves. Plant Cell Environ. 16, 587–591 10.1111/j.1365-3040.1993.tb00907.x
39. Schnitzler JP, Graus M, Kreuzwieser J, Heizmann U, Rennenberg H, Wisthaler A et al. (2004) Contribution of different carbon sources to isoprene biosynthesis in poplar leaves. Plant Physiol. 135, 152–160 10.1104/pp.103.037374 [PubMed: 15122010]
40. Karl T, Fall R, Rosenstiel TN, Prazeller P, Larsen B, Seufert G et al. (2002) On-line analysis of the $^{13}CO_2$ labeling of leaf isoprene suggests multiple subcellular origins of isoprene precursors. Planta 215, 894–905 10.1007/s00425-002-0825-2 [PubMed: 12355149]
41. Loreto F, Ciccioli P, Brancaleoni E, Cecinato A, Frattoni M and Sharkey TD (1996) Different sources of reduced carbon contribute to form three classes of terpenoid emitted by Quercus ilex L leaves. Proc. Nat. Acad. Sci. U.S.A 93, 9966–9969 10.1073/pnas.93.18.9966
42. Trowbridge AM, Asensio D, Eller AS, Way DA, Wilkinson MJ, Schnitzler JP et al. (2012) Contribution of various carbon sources toward isoprene biosynthesis in poplar leaves mediated by altered atmospheric CO_2 concentrations. PLoS One 7, e32387 10.1371/journal.pone.0032387 [PubMed: 22384238]
43. Guidolotti G, Pallozzi E, Gavrichkova O, Scartazza A, Mattioni M, Loreto F et al. (2019) Emission of constitutive isoprene, induced monoterpenes and other volatiles under high temperatures in Eucalyptus camaldulensis. a ^{13}C labelling study. Plant Cell Environ. 42, 1929–1938 10.1111/pce.13521 [PubMed: 30663094]
44. Brilli F, Barta C, Fortunati A, Lerdau M, Loreto F and Centritto M (2007) Response of isoprene emission and carbon metabolism to drought in white poplar (Populus alba) saplings. New Phytol. 175, 244–254 10.1111/j.1469-8137.2007.02094.x [PubMed: 17587373]
45. Yáñez-Serrano AM, Mahlau L, Fasbender L, Byron J, Williams J, Kreuzwieser J et al. (2019) Heat stress causes enhanced use of cytosolic pyruvate for isoprene biosynthesis. J. Exp. Bot 70, 5827–5838 10.1093/jxb/erz353 [PubMed: 31396620]
46. de Souza VF, Niinemets ʊ., Rasulov B, Vickers CE, Duvoisin Junior S, Araujo WL et al. (2018) Alternative carbon sources for isoprene emission. Trends Plant Sci 23, 1081–1101 10.1016/jrtplants.2018.09.012 [PubMed: 30472998]
47. Jardine K, Chambers J, Alves EG, Teixeira A, Garcia S, Holm J et al. (2014) Dynamic balancing of isoprene carbon sources reflects photosynthetic and photorespiratory responses to temperature stress. Plant Physiol. 166, 2051–2064 10.1104/pp.114.247494 [PubMed: 25318937]
48. Hoagland DR and Arnon DI (1938) The water culture method for growing plants without soil. Circ. Calif. Agric. Exp. Stn 347, 1–39
49. Schrader SM, Kleinbeck KR and Sharkey TD (2007) Rapid heating of intact leaves reveals initial effects of stromal oxidation on photosynthesis. Plant Cell Environ. 30, 671–678 10.1111/j.1365-3040.2007.01657.x [PubMed: 17470143]
50. Guenther AB and Hills AJ (1998) Eddy covariance measurement of isoprene fluxes. J. Geophys. Res 103, 13, 145–13, 152 10.1029/97JD03283
51. Lunn JE, Feil R, Hendriks Janneke HM, Gibon Y, Morcuende R, Osuna D et al. (2006) Sugar-induced increases in trehalose 6-phosphate are correlated with redox activation of ADPglucose pyrophosphorylase and higher rates of starch synthesis inArabidopsis thaliana. Biochem. J 397, 139–148 10.1042/BJ20060083 [PubMed: 16551270]
52. Cocuron J-C and Alonso AP (2014) Liquid chromatography tandem mass spectrometry for measuring ^{13}C-labeling in intermediates of the glycolysis and pentose phosphate pathway. Methods Mol. Biol. (Clifton, N.J.) 1090, 131–142 10.1007/978-1-62703-688-7_9
53. Weise SE, Liu T, Childs KL, Preiser AL, Katulski HM, Perrin-Porzondek C et al. (2019) Transcriptional regulation of the glucose-6-phosphate/ phosphate translocator 2 is related to carbon exchange across the chloroplast envelope. Front. Plant Sci 10, 827 10.3389/fpls.2019.00827 [PubMed: 31316533]

54. Kammerer B, Fischer K, Hilpert B, Schubert S, Gutensohn M, Weber A et al. (1998) Molecular characterization of a carbon transporter in plastids from heterotrophic tissues: the glucose 6-phosphate phosphate antiporter. Plant Cell 10,105–117 10.1105/tpc.10.1.105 [PubMed: 9477574]
55. Hilgers EJA, Staehr P, FlQgge U-I and Hausler RE (2018) The xylulose 5-phosphate/phosphate translocator supports triose phosphate, but not phosphoenolpyruvate transport across the inner envelope membrane of plastids in Arabidopsis thaliana mutant plants. Front. Plant Sci 9, 1461 10.3389/fpls.2018.01461 [PubMed: 30405650]
56. Eicks M, Maurino V, Knappe S, FlQgge U-I and Fischer K (2002) The plastidic pentose phosphate translocator represents a link between the cytosolic and the plastidic pentose phosphate pathways in plants. Plant Physiol. 128, 512–522 10.1104/pp.010576 [PubMed: 11842155]
57. Preiser AL, Fisher N, Banerjee A and Sharkey TD (2019) Plastidic glucose-6-phosphate dehydrogenases are regulated to maintain activity in the light. Biochem. J 476, 1539–1551 10.1042/BCJ20190234 [PubMed: 31092702]
58. Loreto F, Define S and Di Marco G (1999) Estimation of photorespiratory carbon dioxide recycling during photosynthesis. Aust. J. Plant Physiol 26, 733–736 10.1071/PP99096
59. González-Cabanelas D, Wright LP, Paetz C, Onkokesung N, Gershenzon J, Rodrfguez-Concepcion M et al. (2015) The diversion of 2-C-methyl-D-erythritol-2,4-cyclodiphosphate from the 2-C-methyl-D-erythritol 4-phosphate pathway to hemiterpene glycosides mediates stress responses in Arabidopsis thaliana. Plant J. 82,122–137 10.1111/tpj.12798 [PubMed: 25704332]
60. Wright LP, Rohwer JM, Ghirardo A, Hammerbacher A, Ortiz-Alcaide M, Raguschke B et al. (2014) Deoxyxylulose 5-phosphate synthase controls flux through the methylerythritol 4-phosphate pathway in Arabidopsis. Plant Physiol. 165, 1488–1504 10.1104/pp.114.245191 [PubMed: 24987018]
61. Xiao Y, Savchenko T, Baidoo EE, Chehab WE, Hayden DM, Tolstikov V et al. (2012) Retrograde signaling by the plastidial metabolite MEcPP regulates expression of nuclear stress-response genes. Cell 149, 1525–1535 10.1016/j.cell.2012.04.038 [PubMed: 22726439]
62. Loreto F, Pinelli P, Brancaleoni E and Ciccioli P (2004) ^{13}C labelling reveals chloroplastic and extra-chloroplastic pools of dimethylallyl pirophosphate and their contribution to isoprene formation. Plant Physiol. 135, 1903–1907 10.1104/pp.104.039537 [PubMed: 15286296]
63. Loreto F, Ciccioli P, Cecinato A, Brancaleoni E, Frattoni M, Fabozzi C et al. (1996) Evidence of the photosynthetic origin of monoterpenes emitted by Quercus ilex L leaves by 13 C labeling. Plant Physiol. 110, 1317–1322 10.1104/pp.110.4.1317 [PubMed: 12226263]
64. Mahon JD, Fock H and Canvin DT (1974) Changes in specific radioactivities of sunflower leaf metabolites during photosynthesis in $^{14}CO_2$ and $^{12}CO_2$ at normal and low oxygen. Planta 120, 125–134 10.1007/BF00384922 [PubMed: 24442651]
65. Allen DK and Young JD (2020) Tracing metabolic flux through time and space with isotope labeling experiments. Curr. Opin. Biotechnol 64, 92–100 10.1016/j.copbio.2019.11.003 [PubMed: 31864070]
66. Ghirardo A, Wright LP, Bi Z, Rosenkranz M, Pulido P, Rodriguez-Concepcion M et al. (2014) Metabolic flux analysis of plastidic isoprenoid biosynthesis in poplar leaves emitting and non-emitting isoprene. Plant Physiol. 165, 37–51 10.1104/pp.114.236018 [PubMed: 24590857]
67. Bassham JA, Benson AA, Kay LD, Harris AZ, Wilson AT and Calvin M (1954) The path of carbon in photosynthesis. XXI. The cyclic regeneration of carbon dioxide acceptor. J. Am. Chem. Soc 76, 1760–1770 10.1021/ja01636a012
68. Gibbs M and Kandler O (1957) Asymmetric distribution of C14 in sugars formed during photosynthesis. Proc. Nat. Acad. Sci. U.S.A 43, 446 10.1073/pnas.43.6.446
69. Cseke C, Balogh A, Wong JH, Buchanan BB, Stitt M, Herzog B et al. (1984) Fructose 2,6-bisphosphate: a regulator of carbon processing in leaves. Trends Biochem. Sci 9, 533–535 10.1016/0968-0004(84)90284-6
70. Stitt M, Herzog B and Heldt HW (1984) Control of photosynthetic sucrose synthesis by fructose-2,6-bisphosphate. I. Coordination of CO_2 fixation and sucrose synthesis. Plant Physiol. 75, 548–553 10.1104/pp.75.3.548 [PubMed: 16663664]
71. Sharkey TD and Weise SE (2012) Autotrophic carbon dioxide fixation In Photosynthesis: Plastid Biology, Energy Conversion and Carbon Assimilation. Advances in Photosynthesis and

Respiration (Eaton-Rye JJ, Tripathy B and Sharkey TD, eds), pp. 649–672, Springer Academic Publications, Dordrecht

72. Li J, Weraduwage SM, Preiser AL, Tietz S, Weise SE, Strand DD et al. (2019) A cytosolic bypass and G6P shunt in plants lacking peroxisomal hydroxypyruvate reductase. Plant Physiol. 180, 783–792 10.1104/pp.19.00256 [PubMed: 30886114]
73. Granot D, Kelly G, Stein O and David-Schwartz R (2014) Substantial roles of hexokinase and fructokinase in the effects of sugars on plant physiology and development. J. Exp. Bot 65, 809–819 10.1093/jxb/ert400 [PubMed: 24293612]
74. Moore B, Zhou L, Rolland F, Hall Q, Cheng WH, Liu YX et al. (2003) Role of the Arabidopsis glucose sensor HXK1 in nutrient, light, and hormonal signaling. Science 300, 332–336 10.1126/science.1080585 [PubMed: 12690200]
75. Sharkey TD and Weise SE (2016) The glucose 6-phosphate shunt around the Calvin–Benson cycle. J. Exp. Bot 67, 4067–4077 10.1093/jxb/erv484 [PubMed: 26585224]
76. Weise SE, Kim KS, Stewart RP and Sharkey TD (2005) β-maltose is the metabolically active anomer of maltose during transitory starch degradation. Plant Physiol. 137, 756–761 10.1104/pp.104.055996 [PubMed: 15665241]
77. Zhang R and Sharkey TD (2009) Photosynthetic electron transport and proton flux under moderate heat stress. Photosyn. Res 100, 29–43 10.1007/s11120-009-9420-8
78. Sharkey TD and Schrader SM (2005) High temperature stress In Phyiology and Molecular Biology of Stress Tolerance in Plants (Rao KVM, Raghavendra AS and Reddy K, eds), pp. 101–129, Springer, The Netherlands
79. Schrader SM, Wise RR, Wacholtz WF, Ort DR and Sharkey TD (2004) Thylakoid membrane responses to moderately high leaf temperature in Pima cotton. Plant Cell Environ. 27, 725–735 10.1111/j.1365-3040.2004.01172.x
80. Bukhov NG, Wiese C, Neimanis S and Heber U (1999) Heat sensitivity of chloroplasts and leaves: Leakage of protons from thylakoids and reversible activation of cyclic electron transport. Photosyn. Res 59, 81–93 10.1023/A:1006149317411
81. Havaux M (1996) Short-term responses of photosystem I to heat stress - Induction of a PS II-independent electron transport through PS I fed by stromal components. Photosyn. Res 47, 85–97 10.1007/BF00017756
82. Strand DD, Livingston AK, Satoh-Cruz M, Froehlich JE, Maurino VG and Kramer DM (2015) Activation of cyclic electron flow by hydrogen peroxide in vivo. Proc. Nat. Acad. Sci. U.S.A 112, 5539–5544 10.1073/pnas.1418223112
83. Sharkey TD and Weise SE (2016) The glucose 6-phosphate shunt around the Calvin–Benson cycle. J. Exp. Bot 67, 4067–4077 10.1093/jxb/erv484 [PubMed: 26585224]

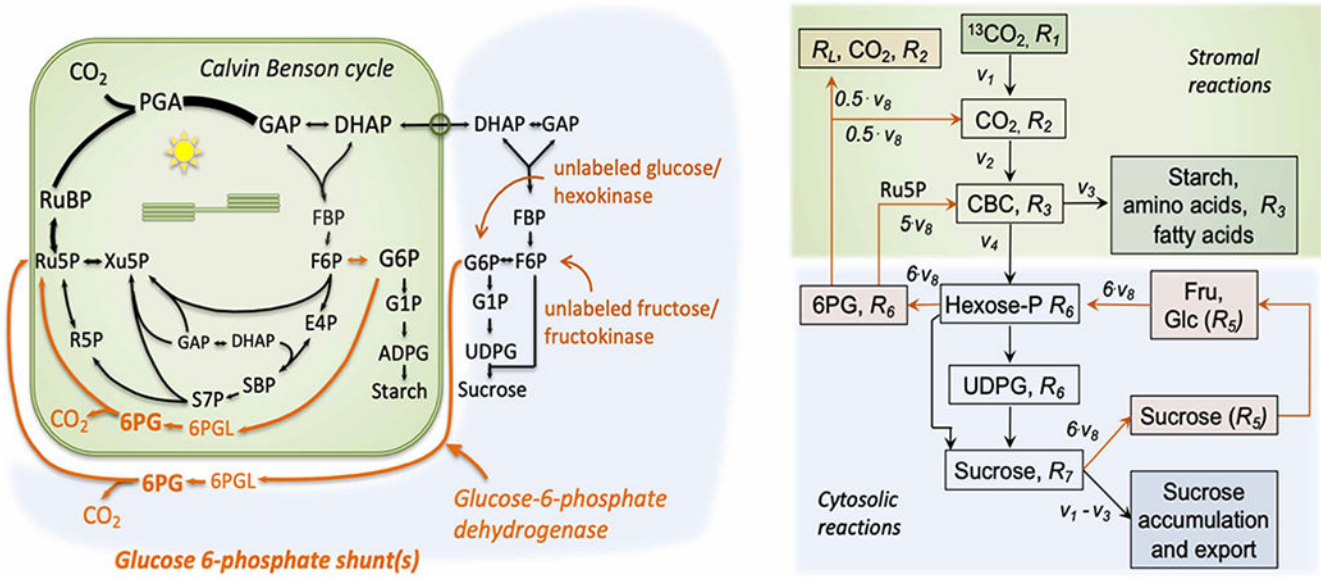

Figure 1. Paths of carbon flow and model to explain the lack of complete labeling of Calvin–Benson cycle intermediates and isoprene.

The Calvin–Benson cycle, starch synthesis, sucrose synthesis, and glucose-6-phosphate shunts are shown on the left while a simplified model to account for changes in the ratio of 13–12 C is shown on the right. Relative velocities, *v*, with net CO_2 fixation set to 1, and ratios of 13–12 C, *R*, are used. Line thickness in the Calvin–Benson cycle (CBC) is related to the relative amount of carbon transiting each reaction. Cytosolic reactions that allow unlabeled carbon to enter the CBC through the cytosolic glucose 6-phosphate shunt [83] are modeled to determine the expected label in UDP glucose (UDPG) given a degree of label in Calvin–Benson cycle intermediates as reported by ADP glucose (ADPG). 6PG, 6 phosphogluconate; DHAP, dihydroxyacetone phosphate; E4P, erythrose 4-phosphate; F6(B)P, fructose 6(bis)-phosphate; G6P, glucose 6-phosphate; GAP, glyceraldehyde 3-phosphate; R5P, ribose 5-phosphate; Ru5P, ribulose 5-phosphate; S7(B)P, sedoheptulose 7(bis)-phosphate; Xu5P, xylulose 5-phosphate; R_L, respiration in the light.

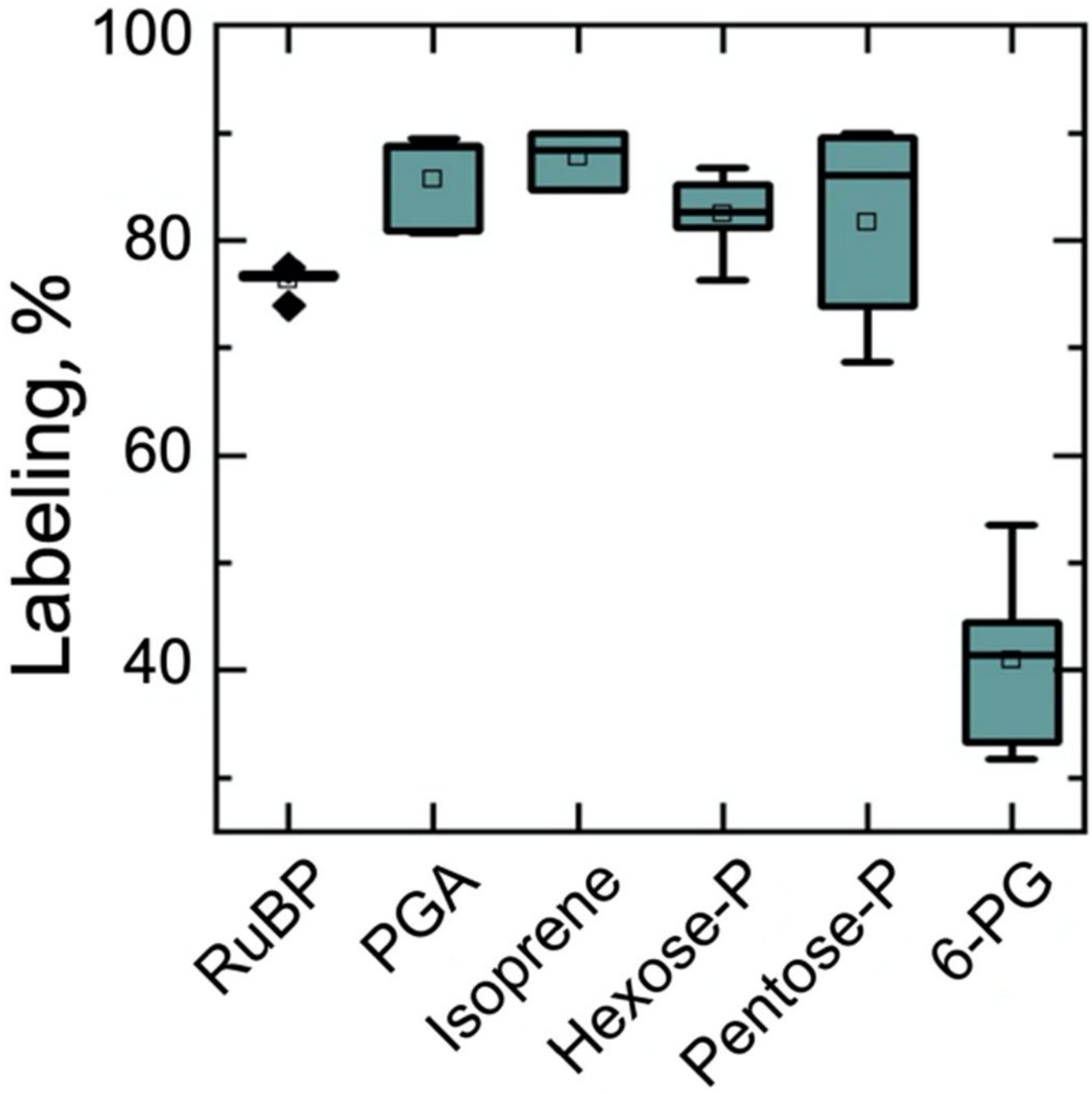

Figure 2. Degree of label in Calvin Benson cycle intermediates, isoprene, and oxidative pentose phosphate pathway intermediate 6-phosphogluconate.

Isoprene labeling is corrected for the unlabeled signals presumed to come from MEcDP exchange between the plastid and cytosol. The horizontal line in the box is the median, the square in the box is the mean, the whiskers show 1.5 times the inter quartile range, the box shows 25–75% of the range, and diamonds show outliers, if any. Hexose-P is glucose 6-phosphate and fructose 6-phosphate and pentose-P is ribulose 5-phosphate and xylulose 5-phosphate.

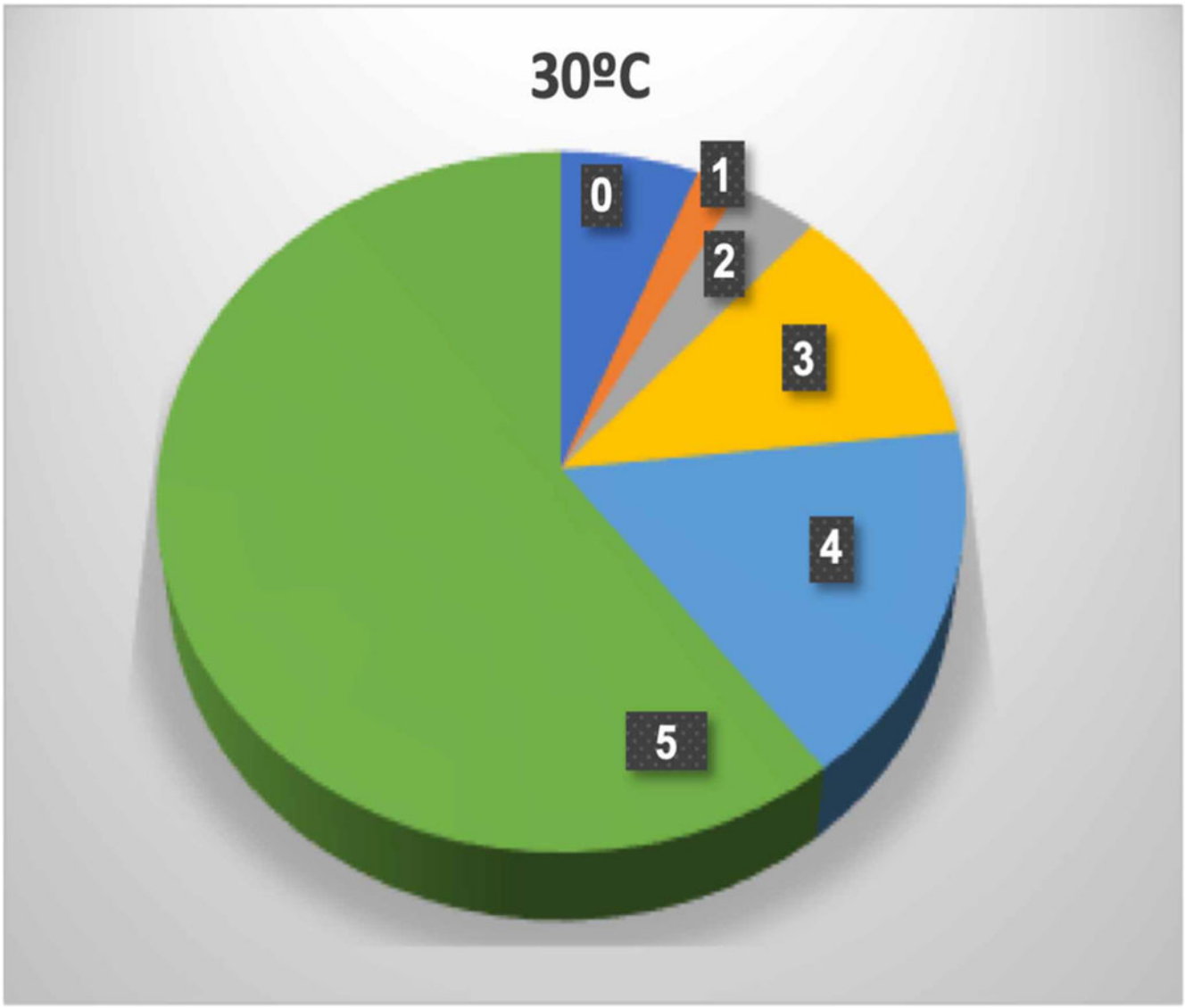

Figure 3. Abundance of isotopologues of isoprene after 20 min of feeding a photosynthesizing leaf with $^{13}CO_2$.

The number on each slice is the number of ^{13}C atoms. The very low degree of label in the singly labeled isotopologue compared with the unlabeled isotopologue may reflect MEcDP exchange between the chloroplast and cytosol.

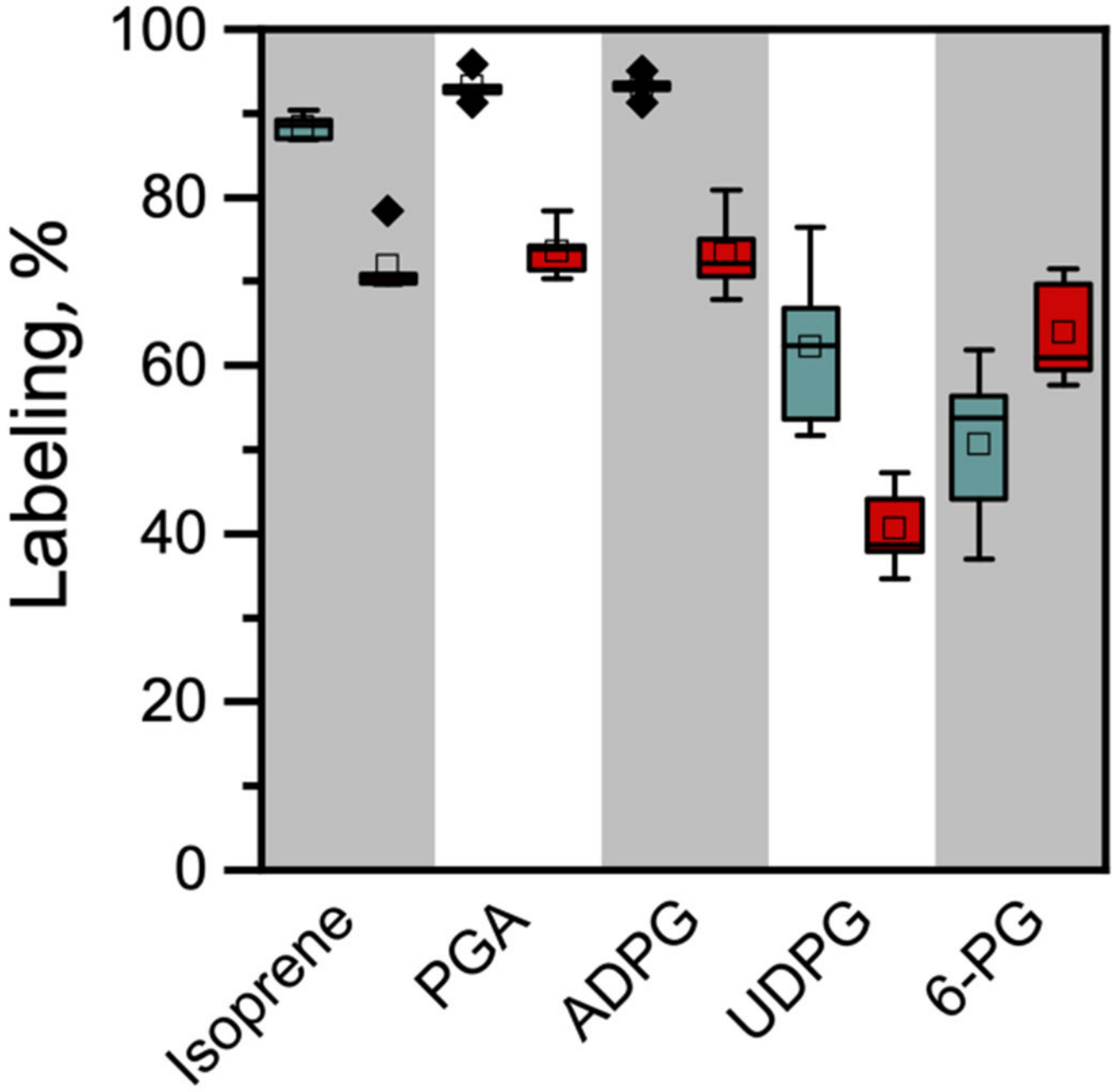

Figure 4. Degree of label (%) of isoprene, PGA, ADPG, UDPG, and 6PG at 30 and 40°C.
Isoprene labeling is corrected for presumed MEcDP exchange with the cytosol. Blue boxes are data from leaves at 30°C while red boxes are data from leaves held at 40°C. ISO, Isoprene; PGA,3-phosphoglycerate; ADPG, ADP glucose, presumed to reflect the glucose- and fructose 6-phosphate pools of the plastids; UDPG, UDP glucose, presumed to reflect the glucose- and fructose 6-phosphate pools of the cytosol; 6PG, 6-phosphogluconate. At 30°C the difference in labeling in UDPG and 6PG is not statistically significant but at 40°C 6PG is significantly more labeled than UDPG.

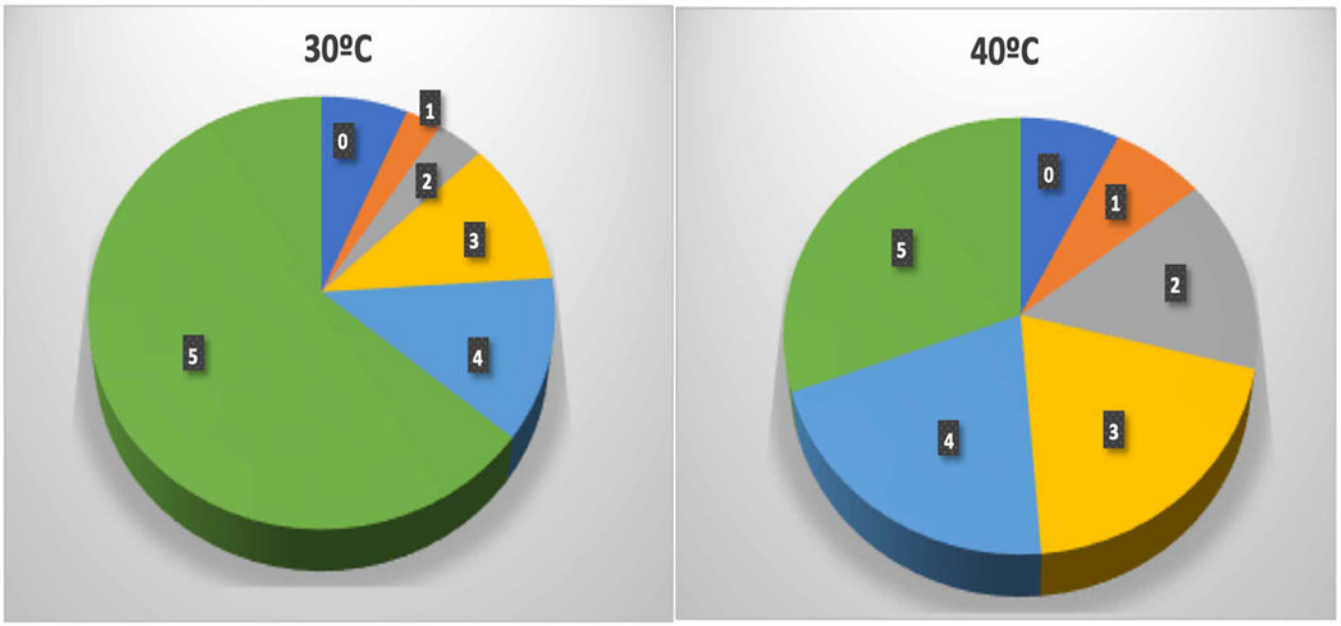

Figure 5. Distribution of isotopologues of isoprene at 30 and 40°C.

The number on each slice is the number of ^{13}C atoms. The unlabeled isotopologue was 6.5 ± 0.8% of the total at 30°C and 7.4 ± 1.2% at 40°C. The difference was not statistically significant (two-tailed *t*-test with unequal variance $P = 0.23$, $n = 5$). If the difference were real it would add 0.9% times 5 carbons of ^{12}C for an effect of 4.5% reduction in label compared with the observed 17.2% decline in label in isoprene at 40°C or about one quarter of the effect if all of the isotopologue zero isoprene at 40°C is from MEcDP. Isotopologue +1 increased from 2.7% at 30°C to 7.0% of total isoprene at 40°C so some of the isotopologue zero isoprene may have resulted from the reduced labeling independent of the MEcDP effect.

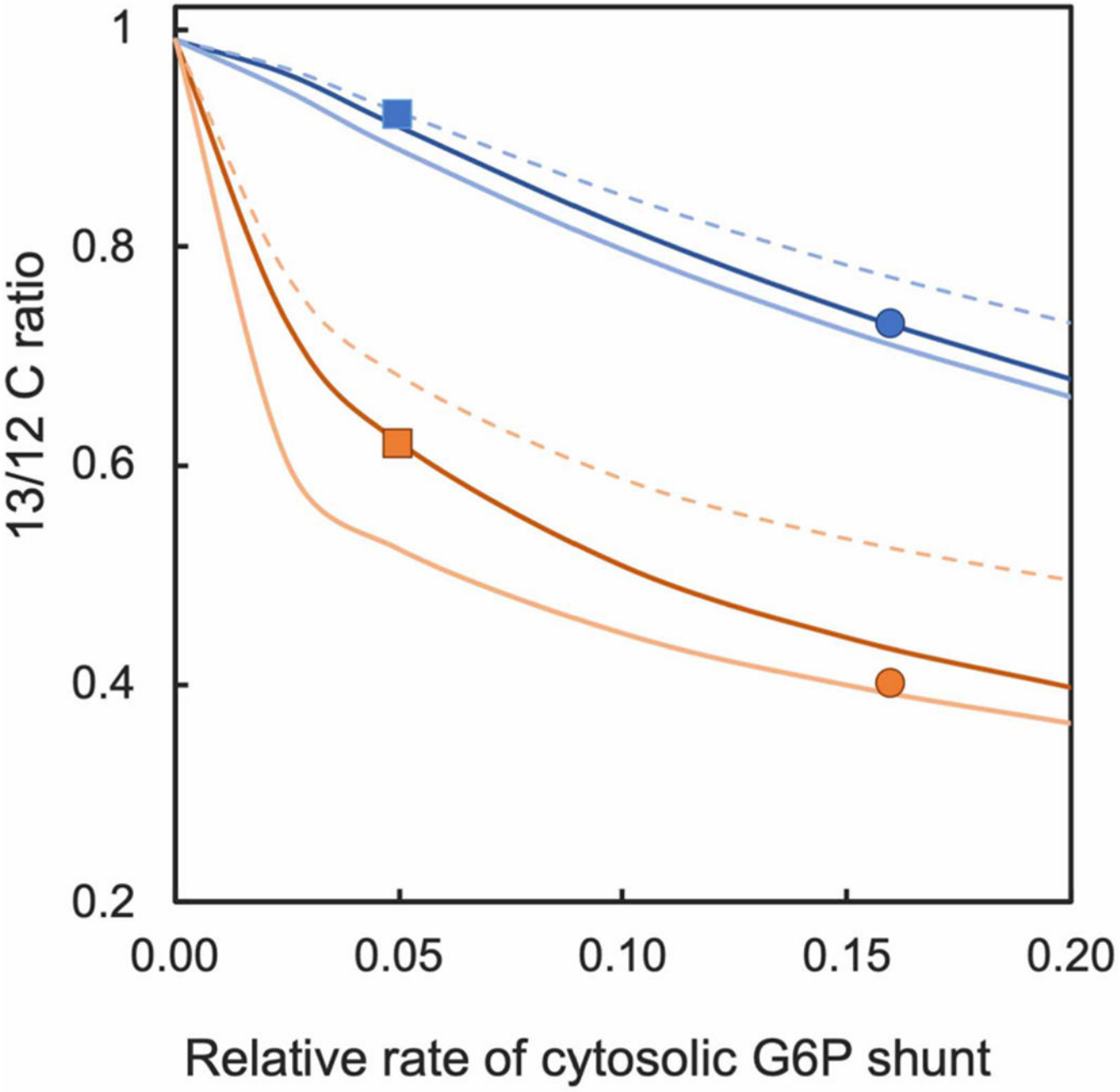

Figure 6. Model output and experimental data.

Lines show how ADP glucose (ADPG) (in blue) and UDP glucose (UDPG) (in orange) vary as a function of the rate of the G6P shunt in the cytosol (relative to net CO_2 assimilation). Data from Figure 4 were placed at a rate determined by the value for ADPG. Squares are data for 30°C and circles are data for 40°C. The dashed lines assume that 30% of carbon fixation is devoted to sucrose synthesis (v_3 in the model = 0.7) and the carbon entering the G6P shunt is 22% labeled (label in sucrose after 20 min of labeling reported by Szecowka et al. [5]). The solid dark lines assume that 30% of carbon fixation is devoted to sucrose synthesis and the carbon entering the G6P shunt is 6.6% labeled (natural abundance ^{13}C

time six carbons). The solid light lines assume that 10% of carbon fixation is devoted to sucrose synthesis (v_3 in the model = 0.9) and the carbon entering the G6P shunt is 6.6% labeled (natural abundance ^{13}C).

Table 1.

Assimilation rate at 30 and 40°C and rate of isoprene emission at 30 and 40°C.

	Assimilation rate (μmol m^{-2} s^{-1})	Isoprene emission rate (nmol m^{-2} s^{-1})	Isoprene/assimilation (%)
30°C	15.8 ± 3.1	20.3 ± 5.6	0.74
40°C	6.6 ± 1.7	54.1 ± 5.0	4.58

Net CO_2 assimilation was reduced at the higher temperature while the rate of isoprene emission was significantly increased. Isoprene emission accounted for 0.7% of net carbon assimilation at 30°C but 4.6% at 40°C. Values are means ± SD, $n = 5$.

Table 2.

Content of hexoses and serine relative to amount needed to account for the slow-to-label CBC intermediates

	Pool size (nmol g^{-1} fr wt)	Pool (nmol C g^{-1} fr wt)	Pool size (minutes)
Glucose	1859	11154	93
Fructose	1058	6348	53
Sucrose	1114	13 368	111
Total			**257**
Serine	1000	3000	25
Organic acids			
Glutamate	1278	6390	53
Malate	761	3044	25
Fumarate	108	432	3.6
Succinate	28	112	0.9

Data are from Szecowka et al. [5] Supplementary Table S1. The rate of photosynthesis was given (Supplementary Figure S7 of Szecowka et al. [5]) as 10 nmol g^{-1} frwt s^{-1}. To keep CBC labeling at 80% would require a dilution at a rate of 2 nmol g^{-1} fr wt s^{-1}. Dividing the pool size in carbon equivalents and dividing by 60 to convert to minutes results in the values in the last column. Glucose plus fructose plus sucrose could supply unlabeled carbon for over 6 h while serine for less than ½ h.